Cell Reports, Volume *34*

Supplemental Information

MCT1 Deletion in Oligodendrocyte Lineage Cells Causes Late-Onset Hypomyelination and Axonal Degeneration

Thomas Philips, Yevgeniya A. Mironova, Yan Jouroukhin, Jeannie Chew, Svetlana Vidensky, Mohamed H. Farah, Mikhail V. Pletnikov, Dwight E. Bergles, Brett M. Morrison, and Jeffrey D. Rothstein

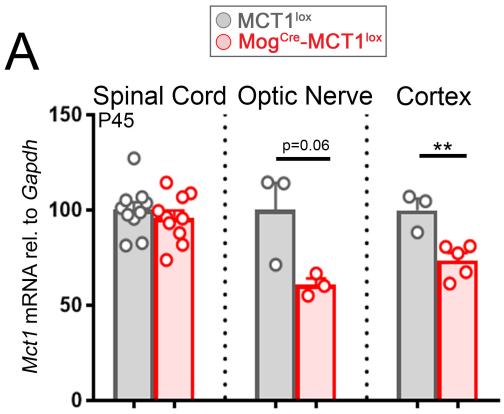
A
MCT1lox
MogCre-MCT1lox
Spinal Cord
Optic Nerve
Cortex
P45
p=0.06
**
Mct1 mRNA rel. to Gapdh
150
100
50
0

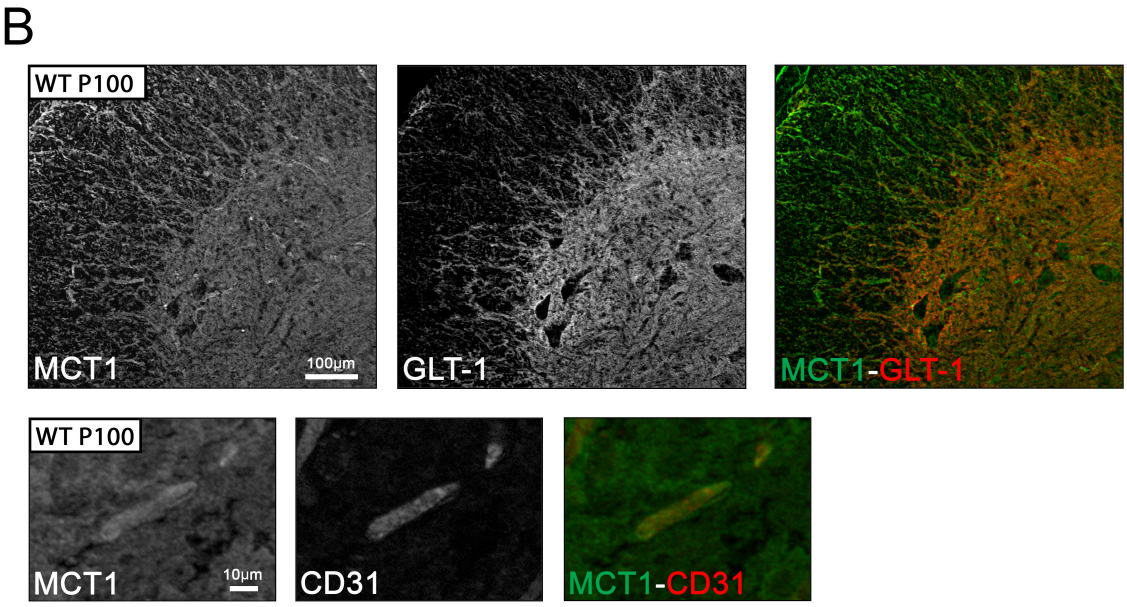
B
WT P100
MCT1
100µm
GLT-1
MCT1-GLT-1
WT P100
MCT1
10µm
CD31
MCT1-CD31

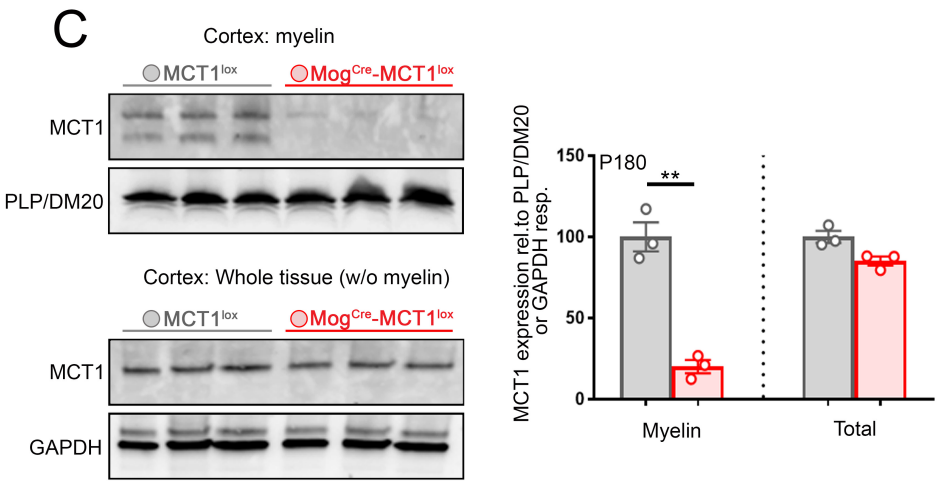
C
Cortex: myelin
MCT1lox
MogCre-MCT1lox
MCT1
PLP/DM20
Cortex: Whole tissue (w/o myelin)
MCT1lox
MogCre-MCT1lox
MCT1
GAPDH
MCT1 expression rel.to PLP/DM20 or GAPDH resp.
P180
**
150
100
50
0
Myelin
Total

Figure S1: Validation of mRNA and protein changes in the Mog^{Cre}-$MCT1^{lox}$ mice and $MCT1^{lox}$ mice and MCT1 antibody immunostaining validation in astrocytes and endothelial cells. Related to Figure 2.

(A) Quantification of *Mct1* mRNA in P45 Mog^{Cre}-$MCT1^{lox}$ and $MCT1^{lox}$ mice in different CNS regions. There is a 26% reduction in *Mct1* mRNA in whole cortex RNA extracts (n=3-10, **p<0.01, Student's t-test). Data is represented as mean ± SEM.

(B) Top panel: Co-Immunolabeling of MCT1 and GLT-1 in astrocytes in the mouse lumbar spinal cord of P100 non-transgenic animals (WT). Bottom panel: Co-immunolabeling of MCT1 and CD31 in endothelial cells in the mouse lumbar spinal cord of P100 non-transgenic animals (WT).

(C) Quantification of MCT1 protein in myelin protein extracts derived from P180 Mog^{Cre}-$MCT1^{lox}$ and $MCT1^{lox}$ cortical tissue. There is an 80% reduction in myelin MCT1 protein expression (n=3, **p<0.01, Student's t-test). Expression in whole tissue (without myelin) was not different between Mog^{Cre}-$MCT1^{lox}$ and $MCT1^{lox}$ mice. Data is represented as mean ± SEM.

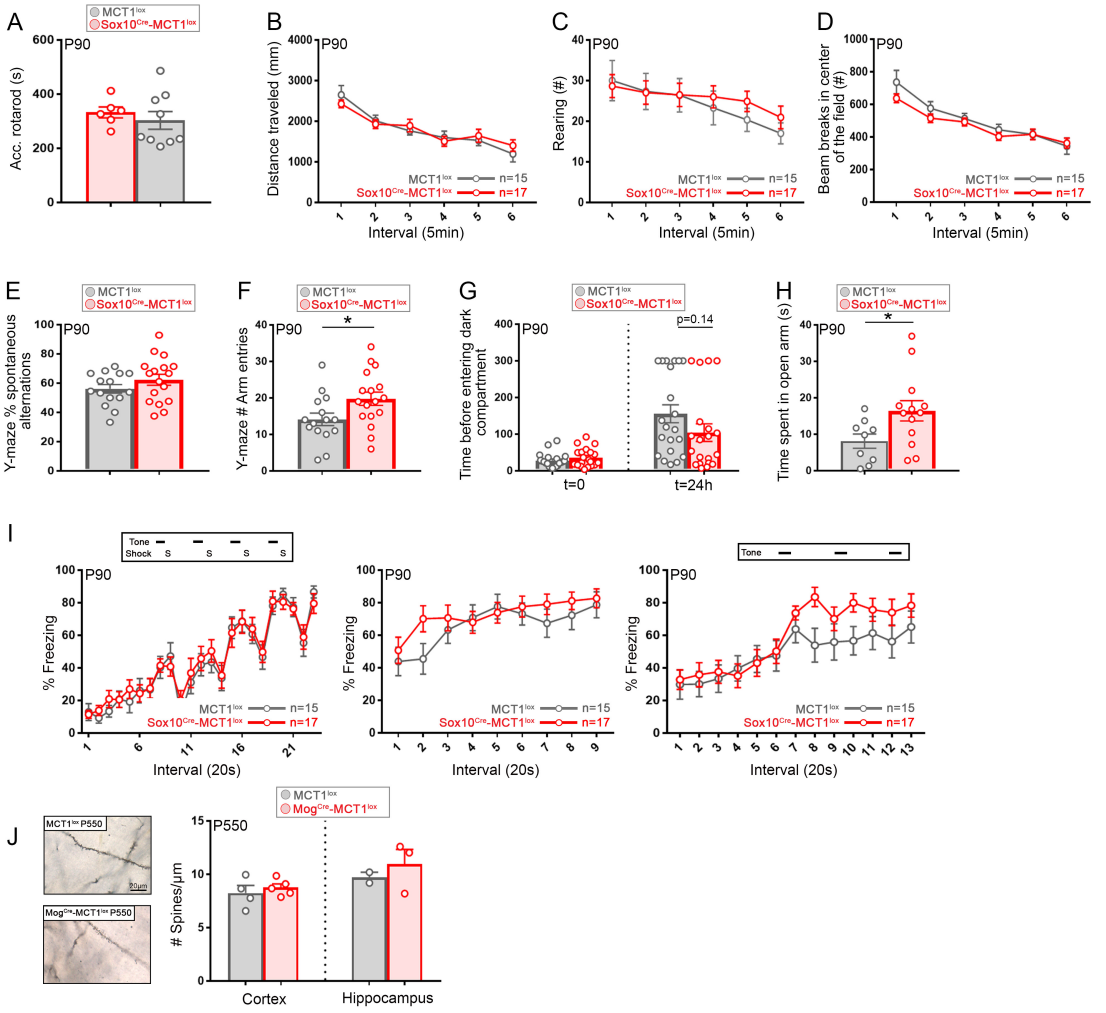

Figure S2: Behavior analysis of P90 Sox10^{Cre}-MCT1^{lox} and MCT1^{lox} littermates control mice. Related to Figure 4.

(A) Accelerated rotarod test does not reveal significant differences between Sox10^{Cre}-MCT1^{lox} and MCT1^{lox} littermates (n=6-9). Data is represented as mean ± SEM.

(B-D) Open field testing does not show any differences in distance travelled (B), rearing (C) and presence in the center versus periphery (D) between $Sox10^{Cre}$-$MCT1^{lox}$ and $MCT1^{lox}$ littermates (n=15-17). Data is represented as mean ± SEM.

(E-F) Working memory assessment in Y-maze does not reveal differences in % spontaneous alternations but showed a 1.4-fold increase in the number of arm entries in the $Sox10^{Cre}$-$MCT1^{lox}$ mice as compared to the $MCT1^{lox}$ controls (n=15-17, *p<0.05, Student's t-test). Data is represented as mean ± SEM.

(G) Passive avoidance test does not reveal differences between $Sox10^{Cre}$-$MCT1^{lox}$ and $MCT1^{lox}$ mice. t=0: the delay for entering a dark compartment after being placed in a brightly lit compartment. The mouse undergoes a 0.5mV shock when entering the dark compartment. t=24h: the delay for each mouse to enter the dark compartment 24 hours after it has been shocked (n=20-21). Data is represented as mean ± SEM.

(H) Time spent in the open arm of the Elevated Plus Maze. There is a 2-fold increase in the percentage of time spent in the open arm in the $Sox10^{Cre}$-$MCT1^{lox}$ as compared to the $MCT1^{lox}$ controls (n=9-13, *p<0.05, Student's t-test). Data is represented as mean ± SEM.

(I) Fear trace conditioning test. Left panel: Training stage: Freezing behavior 24 hours after being preconditioned in the same environment. Mice were exposed to a 90dB tone for 20 seconds for 4 consecutive times. All 4 tones were followed by a 0.5 mV shock for 2 seconds. Middle panel: Context phase: Freezing behavior in the same environment as where the mouse was shocked 24 hours earlier. Right panel: Cued phase: Freezing behavior after hearing 3 bouts of the same tone as in the training phase. The mouse has been placed in a different environment as compared to the earlier phases. There

are no significant differences in freezing behavior at any stage between the Sox10^{Cre}-MCT1^{lox} and MCT1^{lox} mice (n=15-17). Data is represented as mean ± SEM.

(J) Spine density measurements in the cortex and hippocampus of P550 Mog^{Cre}-MCT1^{lox} and MCT1^{lox} littermate controls reveal no significant differences (n=2-5). Data is represented as mean ± SEM.

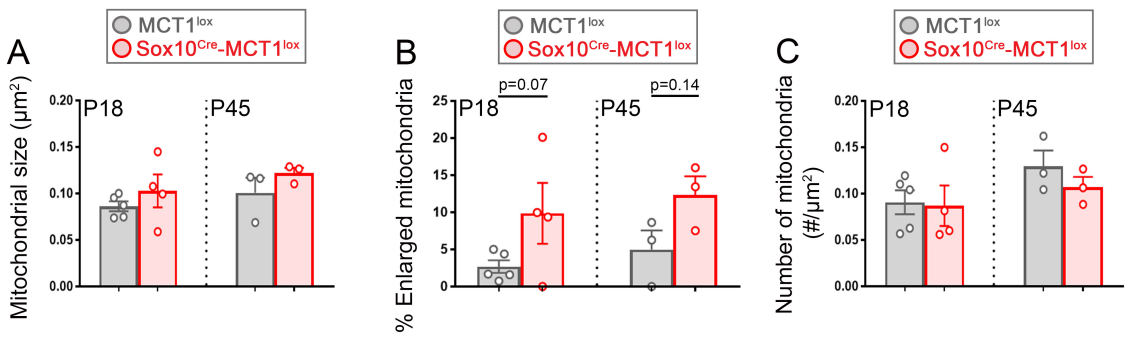
A
MCT1lox
Sox10Cre-MCT1lox
Mitochondrial size (µm²)
P18
P45
B
% Enlarged mitochondria
p=0.07
p=0.14
C
Number of mitochondria (#/µm²)

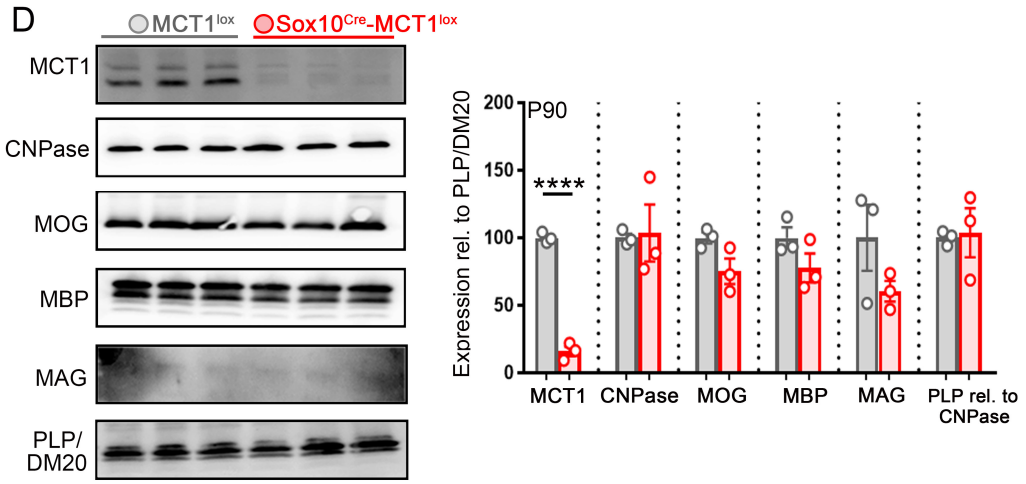
D
MCT1lox
Sox10Cre-MCT1lox
MCT1
CNPase
MOG
MBP
MAG
PLP/
DM20
P90
****
Expression rel. to PLP/DM20
MCT1
CNPase
MOG
MBP
MAG
PLP rel. to CNPase

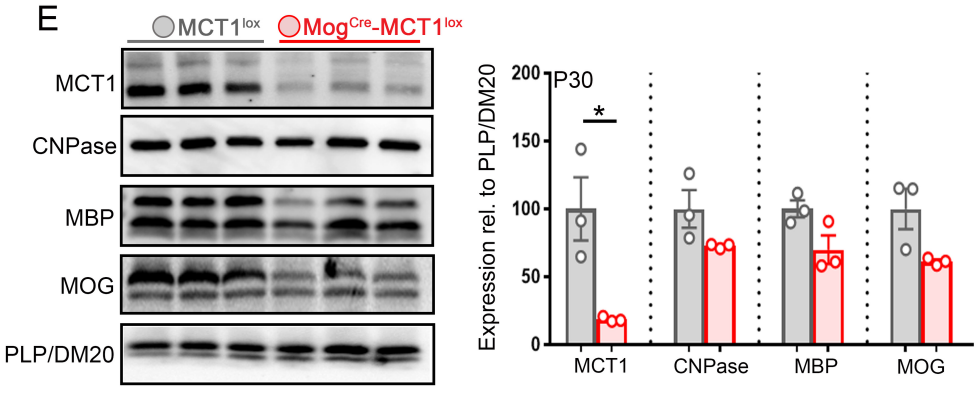
E
MCT1lox
MogCre-MCT1lox
MCT1
CNPase
MBP
MOG
PLP/DM20
P30
*
Expression rel. to PLP/DM20
MCT1
CNPase
MBP
MOG

Figure S3: Analysis of mitochondrial size in P18 and P45 Sox10^{Cre}-MCT1^{lox} mice and myelin protein expression in early adult Sox10^{Cre}-MCT1^{lox}, Mog^{Cre}-MCT1^{lox} mice compared to MCT1^{lox} mice. Related to Figure 4.

(A-B) Analysis of electron microscopic images of optic nerve axons indicates there is no difference in mitochondrial size (A) or % of enlarged mitochondria (>0.20um^2, B) between Sox10^{Cre}-MCT1^{lox} and MCT1^{lox} mice at either P18 or P45 (n=3-5). Data is represented as mean ± SEM.

(C) Analysis of electron microscopic images of optic nerve axons indicates there is no difference in the number of mitochondria when comparing Sox10^{Cre}-MCT1^{lox} and MCT1^{lox} mice at either P18 or P45 (n=4-5). Data is represented as mean ± SEM.

(D) Changes in expression of myelin proteins in cortical myelin protein extracts derived from P90 Sox10^{Cre}-MCT1^{lox} and MCT1^{lox} control mice. There is an 84% reduction in expression of MCT1 whereas expression of CNPase, MBP, MOG and MAG was unchanged as compared to MCT1^{lox} controls (n=3, ****p<0.0001, Student's t-test). Data is represented as mean ± SEM.

(E) Changes in expression of myelin proteins in spinal cord myelin protein extracts derived from P30 Mog^{Cre}-MCT1^{lox} and MCT1^{lox} control mice. There is an 81% reduction in expression of MCT1 while the expression of MOG, CNPase and MBP was unchanged as compared to MCT1^{lox} controls (n=3, *p<0.05, Student's t-test). Data is represented as mean ± SEM.

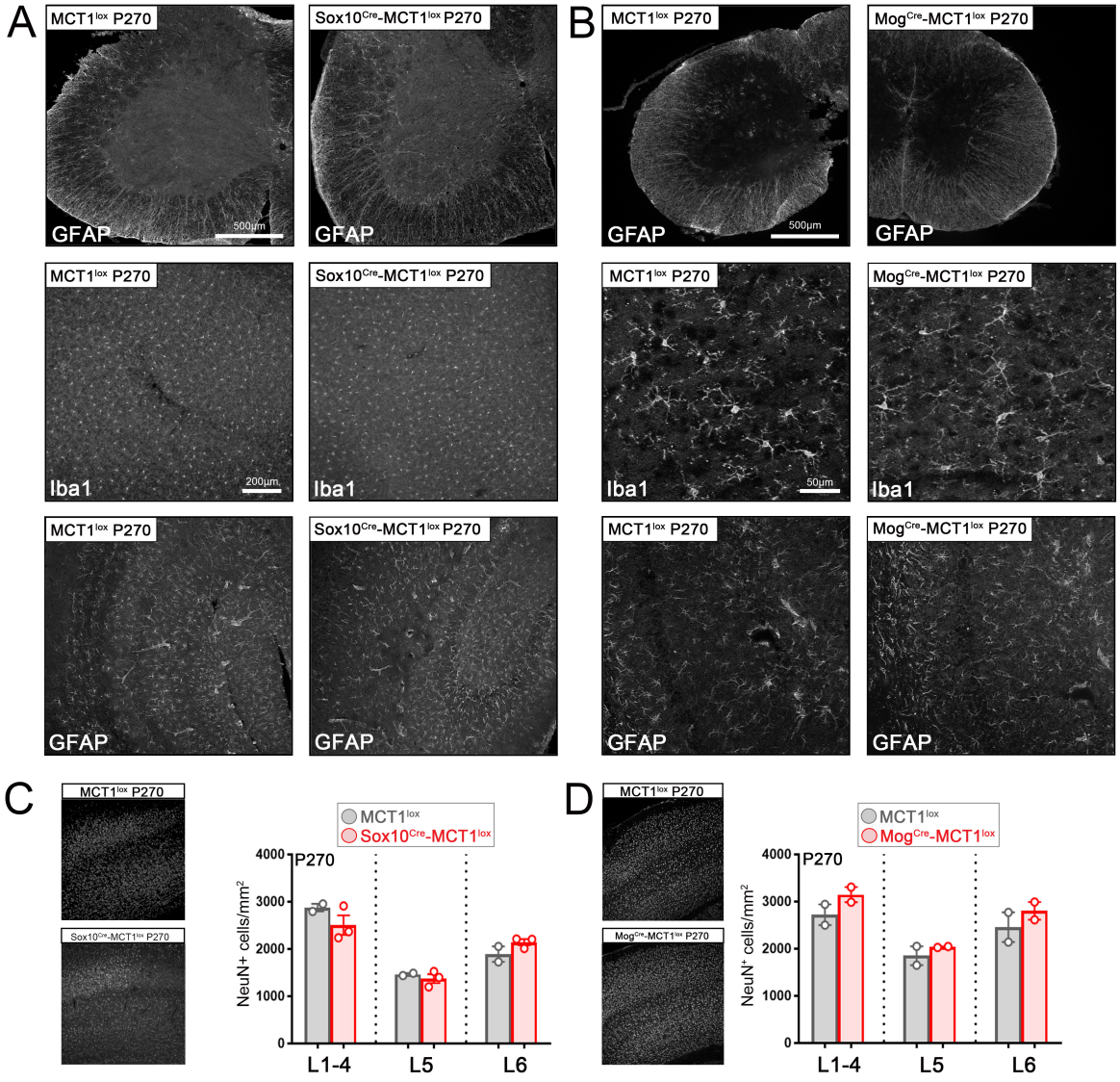

Figure S4: Glial reactivity and neuronal cell density measurements in spinal cord, cortex and hippocampus of P270 Sox10^{Cre}-MCT1^{lox}, Mog^{Cre}-MCT1^{lox} and MCT1^{lox} mice. Related to Figure 5 and Figure 6.

(A) GFAP and Iba1 immunostaining in the lumbar spinal cord (top panel), cortex (middle panel) and hippocampus (lower panel) does not reveal changes in glial reactivity when comparing P270 $Sox10^{Cre}$-$MCT1^{lox}$ and $MCT1^{lox}$ controls.

(B) GFAP and Iba1 immunostaining in the cervical spinal cord (top panel), cortex (middle panel) and hippocampus (lower panel) does not reveal changes in glial reactivity when comparing P270 Mog^{Cre}-$MCT1^{lox}$ and $MCT1^{lox}$ controls.

(C) There is no difference in the number of $NeuN^{+}$ neurons quantified in the cortex layer 1-4 (L4), layer 5 (L5) and layer 6 (L6) in P270 $Sox10^{Cre}$-$MCT1^{lox}$ and $MCT1^{lox}$ controls (n=2-3). Data is represented as mean ± SEM.

(D) There is no difference in the number of $NeuN^{+}$ neurons quantified in the cortex layer 1-4 (L4), layer 5 (L5) and layer 6 (L6) in P270 Mog^{Cre}-$MCT1^{lox}$ and $MCT1^{lox}$ controls (n=2). Data is represented as mean ± SEM.

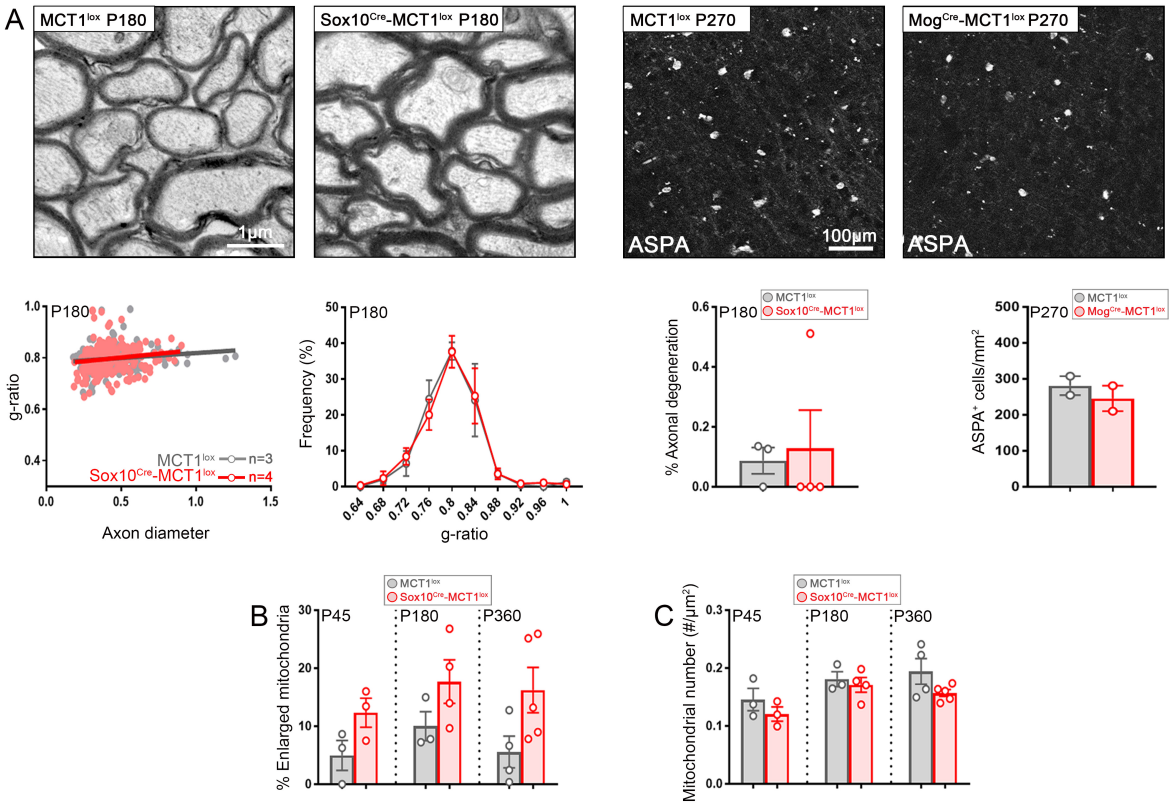

Figure S5: Evaluation of myelin thickness, oligodendrocyte cell counts and mitochondrial size in P45-P360 Sox10^{Cre}-MCT1^{lox}, Mog^{Cre}-MCT1^{lox} and MCT1^{lox} mice. Related to Figure 5 and Figure 6.

(A) Left panels: Electron microscopy images from the optic nerves form P180 Sox10^{Cre}-MCT1^{lox} and MCT1^{lox} controls. There is no axonal pathology and no change in myelin thickness (g-ratio) is observed (n=3-4). Right panels: Immunostaining of ASPA^{+} oligodendrocytes counted in the cortex of P270 Mog^{Cre}-MCT1^{lox} and MCT1^{lox} controls. The number of oligodendrocytes was not different between the two groups (n=2). Data is represented as mean ± SEM.

(B) There are no differences in the percentage of enlarged mitochondria (>0.20µm^2) as observed on electron microscopy images taken from optic nerves dissected from P45, P180 and P360 old Sox10^{Cre}-MCT1^{lox} and MCT1^{lox} mice (n=3-5). Data is represented as mean ± SEM.

(C) There are no differences in the number of mitochondria (per μm^2) measured on electron microscopy images taken from optic nerves dissected from P45, P180 and P360 old $Sox10^{Cre}$-$MCT1^{lox}$ and $MCT1^{lox}$ mice (n=3-5). Data is represented as mean ± SEM.

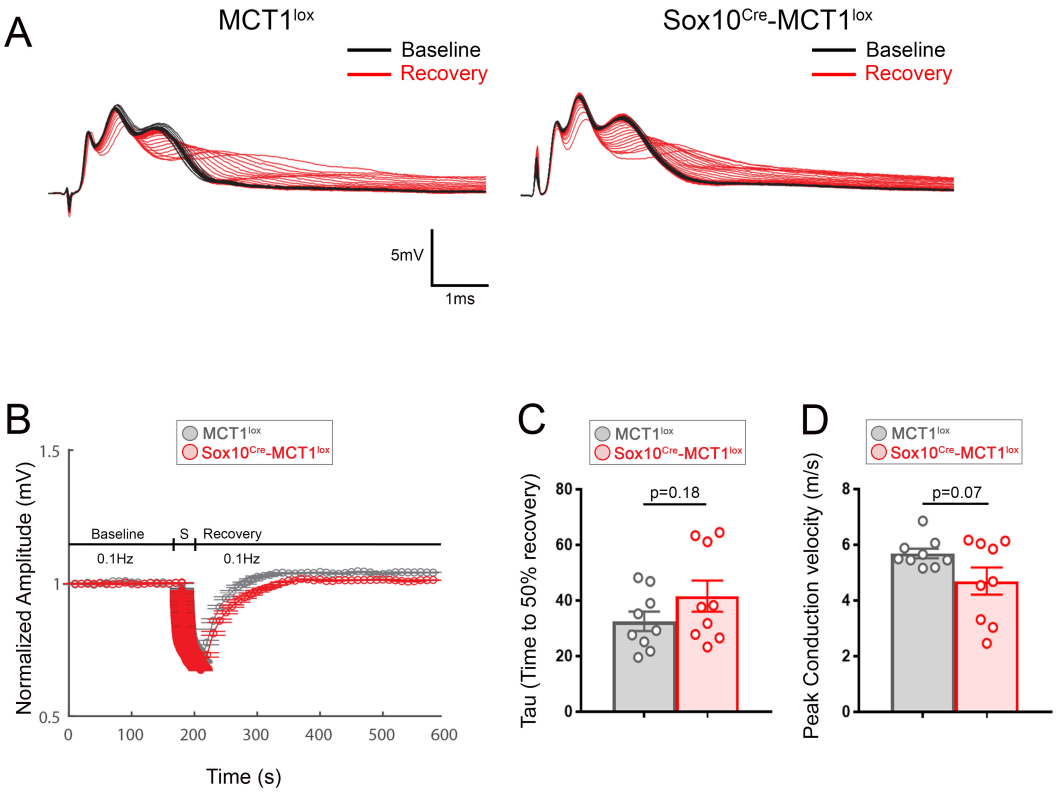

Figure S6: Optic nerve electrophysiological recordings from P360 Sox10^{Cre}-MCT1^{lox} and MCT1^{lox} optic nerves. Related to Figure 6.

(A) Electrophysiological recording traces at baseline (black line) and during recovery (red line) in optic nerves isolated from either P360 MCT1^{lox} (left panel) or P360 Sox10^{Cre}-MCT1^{lox} (right panel) mice (n=9).

(B) Normalized peak amplitude at baseline (0.1Hz stimulation), during a 30 sec. high frequency stimulation (100Hz) (S) and during 5 min. recovery (0.1Hz) in P360 MCT1^{lox} and Sox10^{Cre}-MCT1^{lox} optic nerves. No significant differences are recorded between the two groups (n=9).

(C) There is no significant difference between P360 MCT1^{lox} and Sox10^{Cre}-MCT1^{lox} optic nerves for Tau recovery time (50% recovery) after a high frequency stimulation burst (n=9). Data is represented as mean ± SEM.

(D) There is no significant difference between P360 MCT1^{lox} and Sox10^{Cre}-MCT1^{lox} optic nerves for peak conduction velocity after electrophysiological stimulation (n=9). Data is represented as mean ± SEM.

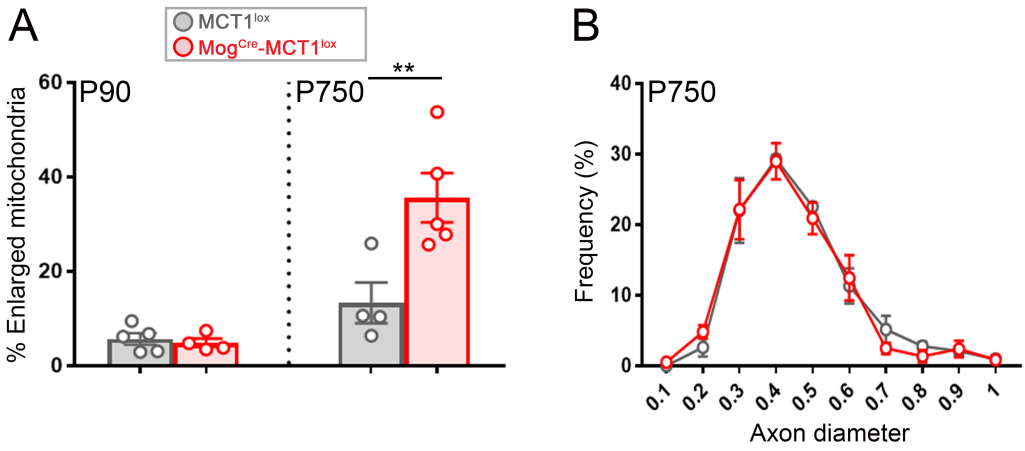

Figure S7: Mitochondrial size and axon size distribution in P750 Mog^{Cre}-MCT1^{lox} and MCT1^{lox} mice. Related to Figure 7.

(A) The percentage of enlarged mitochondria was unchanged in P90 Mog^{Cre}-MCT1^{lox} but increased 2.7-fold in P750 optic nerves dissected from Mog^{Cre}-MCT1^{lox} and MCT1^{lox} controls (n=4-5, **p<0.01, two-way ANOVA with Sidak's multi-comparison test). Data is represented as mean ± SEM.

(B) There is no change in axon size distribution between P750 Mog^{Cre}-MCT1^{lox} and MCT1^{lox} controls (n=4-5). Data is represented as mean ± SEM.

Study	Output	n	Results
Accelerated Rotarod	Motor performance	6-9	n.s. p=0.51
Open Field	General locomotor Activity - Distance traveled - Speed - Rearing - Cen vs Per	15-17	 n.s. p=0.96 n.s. p=0.63 n.s. p=0.69 n.s. p=0.42
Catwalk	Gait, balance, stride - Stride length	6-9	 n.s. p=0.32
Elevated Plus Maze	Anxiety	9-13	*p<0.05
Y maze spontaneous alternations	Working memory - Spontaneous alternations - Arm entries	15-17	 n.s. p=0.21 *p<0.05
Passive avoidance test	Learning/memory (fear)	20-21	n.s. p=0.14
Fear Trace conditioning	Learning/memory (fear) - Context - Cued	15-17	 n.s. p=0.76 n.s. p=0.68

Table S1: Overview of the different animal behavior studies performed on P90 Sox10^{Cre}-MCT1^{lox} and MCT1^{lox} mice. Related to Supplemental Figure 2.

Mct1 het mice	Sox10^{Cre}-MCT1^{lox} mice	Mog^{Cre}-MCT1^{lox} mice
Optic nerve axonopathy by P240	Axonal degeneration by P360	No axonal degeneration by P360 Prominent axonal degeneration by P750
Enhanced glial reactivity by P240 in cortex and hippocampus	Enhanced microglial reactivity by P360, no change in astrocyte reactivity	No changes in glial reactivity up to P270
No myelin deficiencies by P240	Hypomyelination by P360	No myelin deficiencies

Table S2: Side by side comparison of observed phenotypes in *Mct1* het mice, Sox10^{Cre}-MCT1^{lox} mice and Mog^{Cre}-MCT1^{lox} mice. Related to Figures 5-7.